Derivation of the out-of-plane behaviour of masonry through homogenization strategies: micro-scale level

Luís C. Silva(1), Paulo B. Lourenço(2) and Gabriele Milani(3)

[1] PhD candidate, Dept. of Civil Engineering, ISISE, University of Minho, Azurém, 4800-058 Guimarães, Portugal. E-mail: luisilva.civil@gmail.com

[2] Full Professor, Dept. of Civil Engineering, ISISE, University of Minho, Azurém, 4800-058 Guimarães, Portugal. E-mail: pbl@civil.uminho.pt

[3] Associate Professor, Department of Architecture, Built environment and Construction engineering (A.B.C.), Technical University in Milan, Piazza Leonardo da Vinci 32, 20133 Milan, Italy. E-mail: gabriele.milani@polimi.it

Keywords: masonry, homogenization, multi-scale, micro-scale, RVE

Abstract

Two simple and reliable homogenized models are presented for the characterization of the masonry behaviour via a representative volume element (RVE) defined at a structural level. An FE micro-modelling approach within a plate formulation assumption (Kirchhoff-Love and Mindlin-Reissner theory) using Cauchy continuum hypotheses and first-order homogenization theory is adopted. Brick units are considered elastic and modelled through quadrilateral finite elements (FEs) with linear interpolation. Mortar joints are assumed to be inelastic and reduced to zero-thickness interface FEs. A multi-surface plasticity model governs the strength envelope of mortar joints. It can reproduce fracture, frictional slip and crushing along the interface elements, hence making possible the prediction of a stepped, toothed or de-bonding failure pattern of masonry.

Validation tests on the homogenized procedures are undertaken to conclude on the correct identification of the elastic stiffness properties, in the ability to reproduce the masonry orthotropic behaviour and the effect of potential pre-compressive states. Furthermore, the approaches are extended to characterize a case study of an English-bond masonry wall. Both the validation and application steps provide excellent results when compared with available experimental and numerical data from the literature. Conclusions on the influence of three-dimensional shear stresses and the effect of potential discontinuities along the thickness direction are also outlined.

The two homogenized approaches are, for the running- and English-bond masonry cases, integrated within a FE code. By providing reliable and low computational cost solutions’, these are particularly suitable to be combined within multi-scale approaches.

1 Introduction

The analysis of the masonry behaviour in terms of strength and deformation modes is still a challenge. Such complexity arises from: (i) the material heterogeneity, because of the staggering between units and mortar joints; (ii) the non-linearity of the material components; and (iii) the existence of planes of weakness which tend to govern the behaviour and damage, because mortar joints are typically less stiff and less resistant than block units [1].

Advanced computational methodologies are being developed and constitute important tools for the analysis of masonry structures [2]. Approaches such as the discrete element method are quite accurate for the study of dry or weak mortar masonry structures and examples of its application can be seen in [3,4]. These follow a large deformations formulation and with a contact updating between block units, which can be rather rigid or deformable. Yet, conducting a dynamic analysis within a 3D problem demands high processing times. Other advanced numerical strategies, such the ones based on the finite element (FE) method are still receiving more attention from the scientific community, being commonly designated as: (i) the direct simulation or the micro-modelling approach, where units and joints are represented individually; (ii) the macro-modelling approach, where masonry is represented as a homogeneous material; and (iii) the multi-scale computational approach. The reader is referred to [2] for a comprehensive overview of such strategies.

The approach proposed in this paper belongs to the so-called multi-scale methods based on the homogenization theory. Homogenization is basically an averaging procedure performed at a micro-scale upon a Representative Volume Element (RVE). On the RVE, a Boundary Value Problem (BVP) is formulated allowing an estimation of the expected average response to be used as constitutive relations at a macro-level. This framework has been used to investigate the behaviour of composites with different natures [5–11] but is also useful for the study of masonry structures [12–18]. Homogenization theory seems the most efficient compromise between micro- and macro-modelling. The use of such an approach is appealing because it allows deriving the macro-behaviour of masonry through the micro-scale characterization and thus considering its texture, components properties and expected micro-failure modes. In this way, the computational burden (in terms of CPU) is significantly reduced if compared with a fully micro-mechanical description of the material, as demonstrated in [19].

The multi-scale finite element computational homogenization methods, see [5,7,10,20–23], typically rely on a micro and macro transition of information and are thus designated as two-scale or FE^2 approaches. The classical models are based on a first-order homogenization scheme and, as its formulation relies on the first gradient of the kinematics field, two main limitations may arise. The first is related to the principle of separation of scales, which enforces the assumption of uniformity upon the macroscopic fields attributed to each RVE. It is known that in macro-regions where high deformation gradients are present, the latter assumption is not totally effective. The second limitation arises from the fact that the lengths of the two scales are not intrinsically considered on this classical formulation and, therefore, mesh-sensitivity issues and loss of ellipticity of the equilibrium [24] tend to appear when softening behaviour of the material is present [25]. The latter demands a regularization process, for instance upon the fracture energy terms [26,27], to guarantee the problem objectivity. In this scope, several extensions of this method were developed trying to overcome these issues. Some authors extended the classical method to a second-order homogenization [28,29], in which the constitutive behaviour is derived from both the classic part and a higher gradient part and thus, linking the length scales. Other researchers developed techniques that possibly permit the enrichment of the kinematical constraints but still allowing for the use of classical constitutive forms. This is achieved preferably through the use of Cosserat continuum models [30–32]. The well-posedness of the macroscale solution is thus achieved independently of the used mesh, even if the assumption of the separation of scales is lost.

The main advantages of the classical FE^2 approaches are twofold: (i) flexibility on the method to be used at a micro-scale, which can be based on the FE-method [10], Fourier series [33,34], on Voronoi method [20] among others; (ii) it does not require any macro-constitutive relation, because the macro-behaviour is totally dependent on the homogenized response derived on the foregoing scale. Nevertheless, the classical FE^2 approaches (in particular the full continuum-FE methods) are still a challenge in the non-linear range [19,25]. The advantages are especially obvious when linear elastic behaviour is assumed but obtaining a micro-scale solution at each load step for each Gauss point may turn the problem prohibitive from a computational point of view. These strategies still have a higher computational cost if compared with a macro-modelling one. So, the authors believe that if one intends to use homogenization strategies for the study of large or more complex structures, the development of techniques to speed up the processing running times is critical.

Some assumptions may be undertaken which can significantly reduce the computational cost of an FE^2 approach. The use of homogenization methods based on the unit-cell theory, first proposed in the elastic range by Hashin & Rosen [35] and in the nonlinear range by Teply & Dvorak [36] through the use of the so-called hexagonal array model, is a possibility. In these methods (see [37]), closed-form expressions are derived at a micro-scale from both equilibrium and compatibility conditions at the RVE. After being solved or formulated these can provide the homogenized quantities or describe phenomenologically the constitutive equations at a macro-scale, see [17,38,39]. The use of closed-formed solutions is, however, not so feasible in the non-linear range, in complex loading cases or in cases where geometrical and physical changes can occur. Another strategy is the use of the so-called adaptive multi-scale methods [40–42], which take advantage of the best of the first-order theory and micro-modelling approach. A first-order homogenized model represents initially the masonry behaviour until a threshold criterion is reached. Such criterion may be able to account for the onset of damage propagation or another high-gradient source. After reaching the threshold, the area of interest is replaced and kept by an explicit microstructural description able to represent the high localized deformation without the ill-posedness of the first-order theory, see [42] for the masonry field application. These numerical models could be a valuable tool due to its computational attractiveness. Many current studies on unreinforced masonry focus on in-plane cases and for quasi-static loading of running-bond masonry and, therefore, more research is required on structural models with other masonry texture and loading conditions, as out-of-plane loads or seismic excitations.

Besides the assumptions undertaken at a micro-scale, there is also the possibility of using simplified but still accurate methods that can be implemented at a macro-scale. The integration of these models within a micro- to macro- homogenized formulation, i.e. where the material constitutive information is transferred in one step from the micro- to the macro-scale, can be very promising especially for the dynamic study of masonry structures. In fact, some proposals can be found in the literature, for instance, the use of limit analysis [43], or the use of discontinuous or discrete FE-models instead of the classical macroscale continuum-FE strategies. Several works demonstrate its accuracy and computational efficiency when applied to in-plane [43] and out-of-plane loaded masonry [31,44–46] but, as well, for masonry structures subjected to dynamic loads [27,47]. The application of these methods is questionable in cases where multiphase couplings may occur, as when thermal or hydro-mechanical effects may exist. Still, the latter can be disregarded to occur in structural oriented problems.

From the above considerations, the general aim of the present study is to formulate two unit-cell homogenized models. For the sake of avoiding a full three-dimensional discretization of the masonry, both homogenized strategies follow plate (but different) element formulations. Its validation is conducted considering experimental and numerical data available in the literature.

oriented for both in- and out-of-plane analysis of unreinforced periodic masonry structures which may be linked with a proper macro-scale model.

The majority of the existing research on masonry deals with running-bond texture within a single-wythe walls case [12,17,18,39,48–50], being the study of English-bond textures somehow under-investigated [47,51]. The novelty of this work is to present two homogenized-based models oriented for both in- and out-of-plane analysis of English-bond masonry structures. Due to its formulation differences, conclusions on the influence of three-dimensional shear stresses and the effect of discontinuities/transversal joints along the masonry thickness can be drawn. In the analysis, both linear and non-linear ranges are accounted, in which masonry orthotropy and full softening behaviour are reproduced (material nonlinearity lumped on mortar joints).

At last, it may be addressed that the procedures are fully integrated within the commercial software DIANA [52] by exploiting its programming features. These are ready to be combined with a FE^2 approach but, noticing the raised issues of full FE-continuum homogenized strategies, especially suitable to be linked with a discrete-FE macro model aiming to obtain reliable results with a quite attractive computational cost.

2 Outline of the approach proposed

Retrieving models at a micro-scale which are both accurate and implementable on simplified two-step procedures is of most importance. On this behalf, two micro-scale homogenized models based on the theory of plates are presented aiming at the characterization of the behaviour of masonry at a cell level. The accuracy of the results is evaluated through the out-of-plane quantities only. Since the in-plane behaviour of the elementary cell is intrinsically considered to derive such quantities, these are not detailed to avoid redundancy.

Three main steps compose the classical procedure of a first-order homogenization scheme [16,53]: (i) the definition and solution of the micro-scale problem; (ii) the micro-to-macro transition; and (iii) the macro-scale problem solution. The present study focuses on the micro-level, being the formulation and solution of the microscopic problem herein presented. Thus, the macro-quantities which serve as input to solve the microscopic problem are considered as known in the theoretical formulation, as depicted in Figure 1. The general homogenization principles followed are exposed next. After the micro-mechanical model's presentation, their validation on linear and nonlinear ranges are discussed for running bond-masonry and extended to a case study of an English-bond masonry wall.

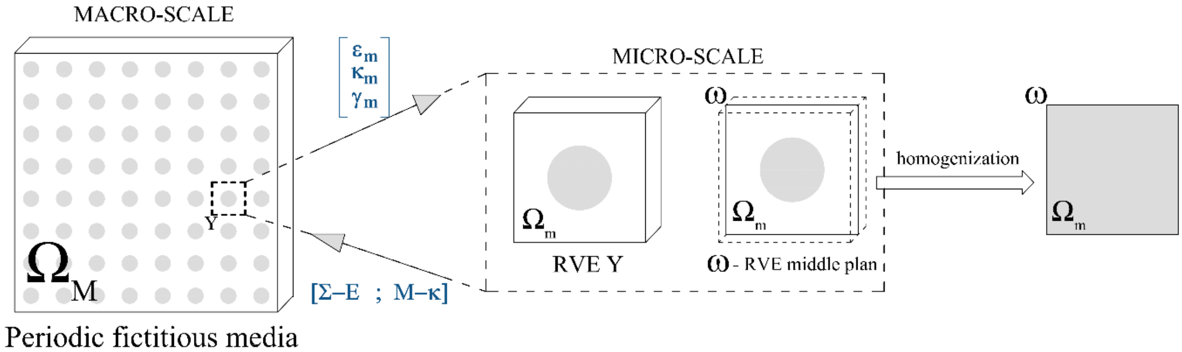

Figure 1 – Work-flow of the proposed unit-cell homogenized models.

3 Microscopic boundary value problem

The theoretical background for the development of the homogenized models is presented in what follows and directly applicable. The numerical models rely on a direct homogenization approach, which involves solving a micro-mechanical problem at a micro-scale and deriving average field variables. This information is then carried out to the macro-scale to constitutively describe the behaviour of the structure.

The definition of a proper RVE is essential, as it may be statistically representative of the body under study. It may accurately embody the heterogeneities of the material and be with a scale length sufficiently small to guarantee the validity of a first-order multi-step procedure. In the case of regular masonry, as running or English bond textures, periodicity is observed both at the micro- and macro-scales. When masonry components do not follow a random distribution but instead a periodic one, it is possible to define only one RVE. The RVE will be discussed next for each considered texture and is herein denoted as Ω_m.

The kinematical description of the homogenized based-models for the in-plane case relies on the assumption that the macroscopic strain tensor $\mathbf{E}$ is obtained as the volume average of the microscopic strain field $\varepsilon_m = \varepsilon_m(y)$ at each point over the associated RVE:

$$\mathbf{E} = \frac{1}{V_m} \int_{\Omega_m} \boldsymbol{\varepsilon}_{\boldsymbol{m}} \, d\mathrm{V} \tag{1}$$

where V_m is the volume of the RVE. The microscopic strain field can be decomposed into a macro-scale and micro-scale contribution. The latter is referred as an additive decomposition of the microscopic strain tensor $\delta\boldsymbol{\varepsilon}_{\boldsymbol{m}} = \delta\boldsymbol{\varepsilon}_{\boldsymbol{m}}(y)$, given as reads:

$$\delta\boldsymbol{\varepsilon}_{\boldsymbol{m}} = \delta\mathbf{E} + \nabla^s u_m \tag{2}$$

where $\delta\mathbf{E}$ is the applied constant strain tensor over the RVE and $\nabla^s u_m$ is the gradient of the fluctuation displacement field. Bearing that $\boldsymbol{\sigma}_m$ is the microscopic stress field, upon RVE equilibrium, the homogenized generalized stress can be derived. The Hill-Mandell principle is based on an energetic equivalence between the macroscopic and microscopic work and allows to address the following relation:

$$\boldsymbol{\Sigma}: \delta\mathbf{E} = \frac{1}{V_m} \int_{\Omega_m} \boldsymbol{\sigma}_m : \delta\boldsymbol{\varepsilon}_{\boldsymbol{m}} \, d\Omega \tag{3}$$

which, according to the assumed additive decomposition of the microscopic strain tensor of Eq. (2), the macro-homogeneity principle reads as:

$$\boldsymbol{\Sigma}: \delta\mathbf{E} = \frac{1}{V_m} \int_{\Omega_m} \boldsymbol{\sigma}_m : \delta\mathbf{E} \, d\Omega + \frac{1}{V_m} \int_{\Omega_m} \boldsymbol{\sigma}_m : \nabla^s \delta u_m \, d\Omega \tag{4}$$

for any kinematical admissible δu_m. Periodic boundary conditions are assumed to solve the BVP. Such consideration is extensively found in homogenization procedures [54], also for the particular case of masonry structures [19,55,56]. The periodic boundary conditions lead to a kinematical field that enforces anti-periodicity of the tractions to occur. The latter is depicted in Figure 2a for the mode-I and horizontal bending mode, which can be mathematically described for any pair of $\{\partial \mathrm{Y_x}^-, \partial \mathrm{Y_x}^+\} \in d\Omega_m$ as:

$$\begin{gathered} \tilde{\mathrm{u}}_{0,\mathrm{m}}\left(\partial \mathrm{Y_x}^+, \mathrm{t}\right) = \tilde{\mathrm{u}}_{0,\mathrm{m}}\left(\partial \mathrm{Y_x}^-, \mathrm{t}\right) \text{, for the in-plane mode-I} \\ \tilde{\mathrm{w}}_{0,\mathrm{m}}\left(\partial \mathrm{Y_x}^+, \mathrm{t}\right) = \tilde{\mathrm{w}}_{0,\mathrm{m}}\left(\partial \mathrm{Y_x}^-, \mathrm{t}\right) \text{, for the horizontal bending of a Kirchhoff-plate theory} \\ \tilde{\theta}_{\mathrm{m}}\left(\partial \mathrm{Y_x}^+, \mathrm{t}\right) = \tilde{\theta}_{\mathrm{m}}\left(\partial \mathrm{Y_x}^-, \mathrm{t}\right) \text{, for the horizontal bending of a Mindlin-plate theory} \end{gathered} \tag{5}$$

Due to the periodicity of the displacement fluctuations on the boundaries, the minimal kinematic constraint required to obtain an admissible microscopic generalized displacement fluctuation is given by Eq. 6:

$$\int_{\Omega_m} \nabla^s \delta u_m \, d\Omega = 0 \tag{6}$$

In this way, Eq. 4 can be simplified and expressed as:

$$\boldsymbol{\Sigma} : \delta\mathbf{E} = \frac{1}{V_m} \int_{\Omega_m} \boldsymbol{\sigma}_m : \delta\mathbf{E} \, d\Omega, \quad \forall \delta\varepsilon \tag{7}$$

Thus, the corollary of the Hill-Mandell principle is that the homogeneous macroscopic stress tensor $\boldsymbol{\sigma}$ can be written as the volume average of the microscopic stress field $\boldsymbol{\sigma}_m = \boldsymbol{\sigma}_m(y)$ over the RVE:

$$\boldsymbol{\Sigma} = \frac{1}{V_m} \int_{\Omega_m} \boldsymbol{\sigma}_m \, d\Omega \tag{8}$$

The variational principle and the use of periodic boundary conditions allow concluding that the external surface traction and body force field in the RVE are reactive terms over the imposed kinematical conditions. These kinematical boundary conditions are dependent on the deformational modes considered on the micro-mechanical level. Thus, the in-plane static equilibrium of the RVE is reached, for each kinematic constraint considered, without any external surface traction and body force terms. The variational principle holds when accounting for the out-of-plane quantities to assure the energy consistency between scales. The difference lies in the replacement of generalized stresses through moment and force terms, as seen in Eq.(9):

$$\mathbf{N}:\delta\mathbf{E}+\mathbf{M}:\delta\boldsymbol{\chi}\;=\frac{1}{V_m}\int_{V_m}\boldsymbol{\sigma}_m\delta\boldsymbol{\varepsilon}_{\boldsymbol{m}}\,dV_m \tag{9}$$

Where $\mathbf{N}$, $\mathbf{M}$ and $\boldsymbol{\chi}$ are the macroscopic membrane force, bending moment and curvature tensors, respectively and $\boldsymbol{\chi}$ is given by Eq. 10:

$$\boldsymbol{\chi}\;=-\frac{1}{V_m}\int_{\Omega_m}u_z\,d\mathrm{V} \tag{10}$$

Note that u_z is the projection of the out-of-plane displacement vector defined by the periodic constraints applied to the RVE. Likewise, if one wants to consider the out-of-plane shear contribution, the term $\mathbf{T}\delta\boldsymbol{\gamma}$ may be added to the left-hand side of the variational principle of Eq. 8, where $\mathbf{T}$ is the macroscopic transverse shear force tensor and $\boldsymbol{\gamma}$ the transverse shear strain vector.

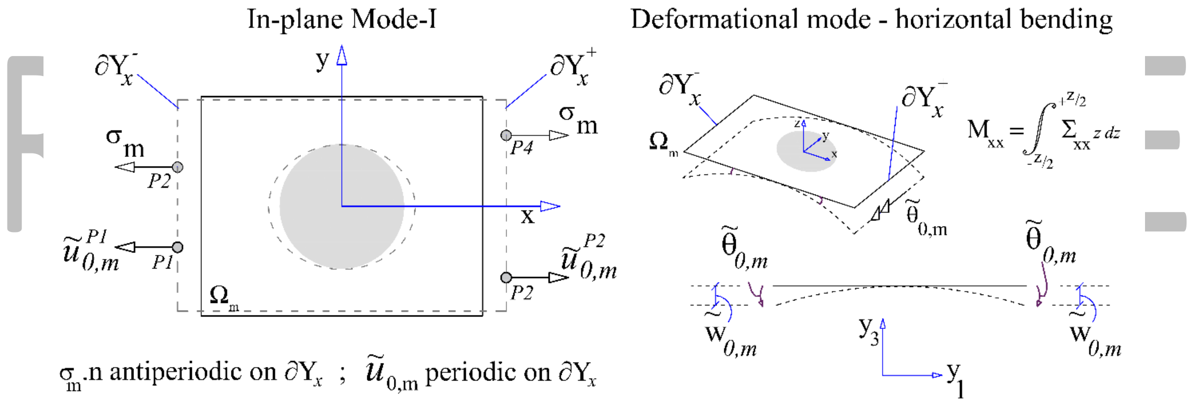

Figure 2 – Representation of the boundary conditions imposed at a micro-scale on a fictitious RVE with double-symmetry: (a) for the in-plane mode-I and (b) for the horizontal bending deformational mode.

4 Nonlinear unit-cell homogenized models

The classical first-order homogenization theory is extended to develop two micro-mechanical models within a strain-driven formulation. Both models have been developed in DIANA by exploiting the software programming capabilities [52] and making use of the available FE library and constitutive material models. A python script has been developed to provide a fully automatic procedure for the modelling, processing and post-processing stages. The proposed homogenized procedures try to cover three features: (i) be capable of studying a representative volume element (RVE) of a given periodic masonry texture; (ii) be accurate on estimating its microscopic linear and nonlinear behaviour, in terms of deformation, stresses and damage propagation; (iii) be adaptable to a FE^2 approach with the aim of estimating the macro-behaviour of a given structure.

The numerical strategies that adopt FE-homogenization schemes typically consider the use of direct numerical simulations. The use of plate models based on a Plane-Stress theory for membrane loading and within a Kirchhoff-Love or Mindlin-Reissner plate theory for out-of-plane load cases may be very attractive [18,19,26,51,57]. These strategies allow reducing the RVE three-dimensional problem to a two-dimensional one, in which the middle plane of the plate ω is considered, and thus obtaining solutions with significant lower computational processing times. However, assuming the media as an infinitely thin membrane may not be the best procedure for problems where three-dimensional shear effects may play an important role. Likewise, if discontinuities are present along the thickness direction (as it is the case of an English masonry bond), considering the material to be homogeneous over the thickness is not so representative. In this context, this study tries to give a contribution about the range of validity of the latter framework and if these can replace a full component description of the material.

To accomplish it, two homogenized–based approaches are presented in what follows for the in- and out-of-plane behaviour characterization. One derives from the Kirchhoff-Love and the other from the Mindlin-Reissner plate theory, see Figure 3. For the sake of conciseness, these models will be designated hereafter as KP and MP model, respectively, and a brief exposition of the key features will be presented only. For extended details on the theoretical background regarding the plates kinematics and constitutive response, the reader is referred to [58–60].

Both KP and MP models are geometrical linear, meaning that the reference plane remains with the initial relative configuration. Instead, material nonlinearity (and cracking) is considered.

4.1 The Kirchhoff-Love plate KP homogenized model

The KP model assumes that at the micro-scale level masonry behaves as a planar 2D continuum, according to a Kirchhoff-Love plate. This is driven by the assumption that the plane section remains normal and straight in relation to the deformed reference plane. The out-of-plane displacement does not vary in the thickness direction and it is assumed that the out-of-plane direct stress component σ_{zz} is negligible. Such hypothesis follows the plane-stress condition. The KP model is thus based on a decoupled characterization between the membrane and bending behaviour, achieved respectively through a plane-stress coupled with a Kirchhoff plate bending model.

The generalized displacement vector for a point of the plate is given as $u = [u_x \quad u_y \quad u_z]^T$, where u_x, u_y are the in-plane and u_z the out-of-plane displacement quantity. The normal strains ε_z are negligible and disregarded. The terms θ_x and θ_y are rotations about the global coordinate system. Basically, according to the elasticity theory, the vector with the unknown quantities of the associated strains is given by $\varepsilon = [\varepsilon_{xx} \quad \varepsilon_{yy} \quad \gamma_{xy} \quad \kappa_{xx} \quad \kappa_{yy} \quad \kappa_{xy}]^T$. Here, the in-plane strains are defined by $\varepsilon_{xx} = \frac{\partial u_x}{\partial x}, \varepsilon_{yy} = \frac{\partial u_y}{\partial y}, \gamma_{xy} = \frac{\partial u_x}{\partial y} + \frac{\partial u_y}{\partial x}$ and the curvature terms of the deflected reference mid-plane as $\kappa_{xx} = \frac{\partial \theta_y}{\partial x}, \kappa_{yy} = \frac{\partial \theta_x}{\partial y}, \kappa_{xy} = \frac{\partial \theta_y}{\partial y} - \frac{\partial \theta_x}{\partial x}$, see Figure 3a. The transverse shear strains are neglected being $\varepsilon_{zz}, \gamma_{xz}, \gamma_{yz} = 0$. The constitutive relation of the homogeneous equivalent material of the RVE is obtained for each deformational in-plane mode considered (Figure 3b), i.e. for the tension (mode-I), in-plane shear (mode-II) and compression (mode IV).

The condition of null out-of-plane shear strains γ_{xz} and γ_{yz} imposed by the Kirchhoff plate theory leads to disregarding their effect on the resultant moments. However, the out-of-plane shear forces Q_x and Q_y are not totally omitted once their contribution is implicitly necessary to fulfil the equilibrium equation of the plate. This highlights why the comparison is performed in terms of coupled stresses-curvature relations.

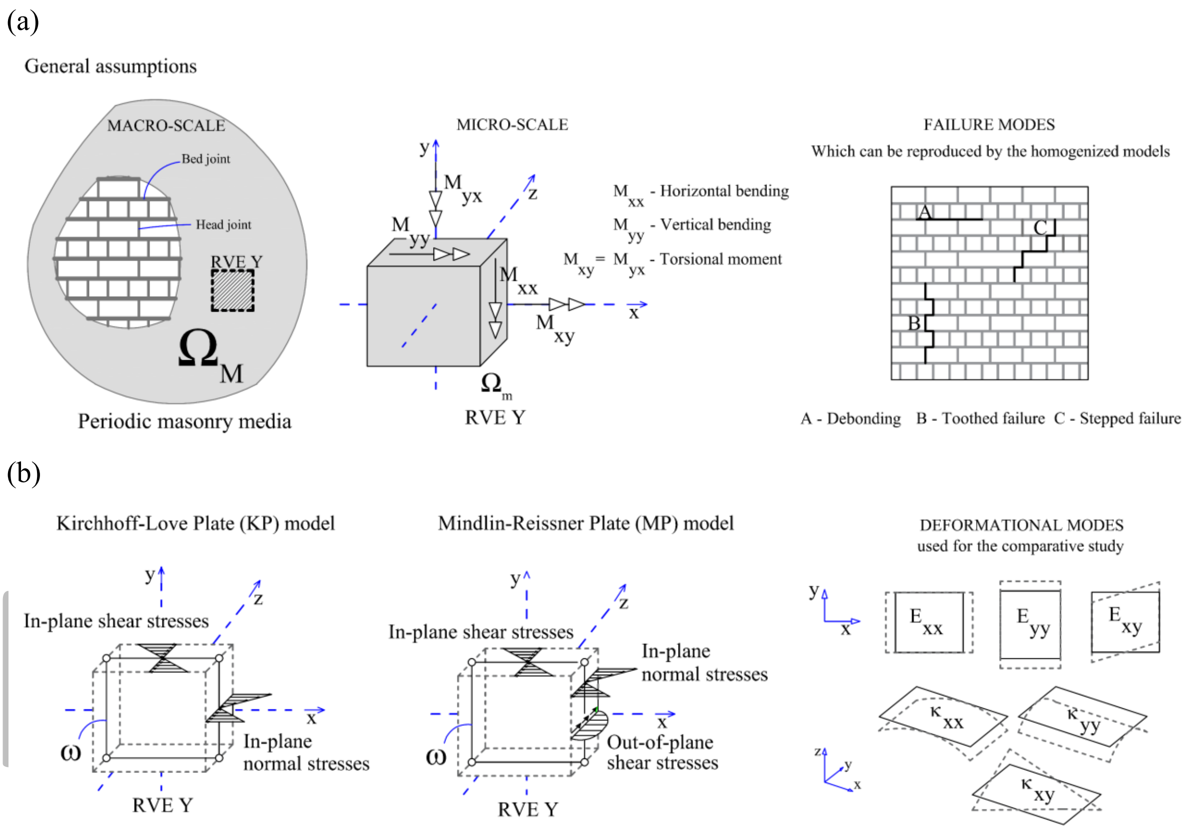

Figure 3 – (a) General assumptions and deformational modes considered for the comparative study between the unit cell homogenization procedures. (b) A brief description of the Kirchhoff-Love and Mindlin-Reissner plate elements and the deformational modes assumed.

4.2 The Mindlin-Reissner plate MP homogenized model

It is well known that in cases where the structure follows a planar behaviour or when the thickness is not relevant (usually referred as 1/10 of the structural dimension), analysing the problem within a two-dimensional approach as the thin plate theory is feasible. Nevertheless, for an out-of-plane loading and in presence of a thick or moderately thick structural element, an enrichment of the latter theory is necessary [58–61]. Such observations are drawn upon a macro-scale level, as for instance [51,61] for the behaviour of masonry structures.

Nevertheless, the investigation of the difference between a three-dimensional model and two-dimensional one (as are the KP and MP models) is still lacking at a micro-scale. Even if the analyses are performed at different scales, the physical behaviour is the same and thus identical conclusions are expected. Still, the authors intend to carry such study to investigate the difference between strategies due to the presence of three-dimensional effects.

In this scope, a strategy based on the first-order shear deformation theory is presented (MP model) which allows including three-dimensional effects, even if in a simplified manner through the out-of-plane shear components and, consequently, increasing both the results accuracy for thick and moderately thick plates with less computational cost than a three-dimensional approach.

Similarly, the membrane behaviour follows a plane-stress element formulation, yet the primary stresses are derived through moments and forces rather than Cauchy stresses. The bending behaviour is decoupled from the latter and follows here the Mindlin-Reissner theory. The in-plane strain quantities (ε_{xx}, ε_{yy}, γ_{xy}) vary in a linear way through the masonry thickness and the transverse shear strains are not disregarded and are derived as $\gamma_{xz} = \frac{\partial u_z}{\partial x} + \theta_y$; $\gamma_{yz} = \frac{\partial u_z}{\partial y} - \theta_x$. Such quantities vary in a parabolic way over the thickness but, for numerical convenience, are assumed as constant within the classical adjustment approach [59]. A shear correction factor equal to $S_r = 1.2$ affects these quantities, in which the equivalent constant shear stress diagrams have an approximate shear strain energy with the actual parabolic behaviour on the area under reference. So, the generalized strain vector is composed by eight unknown parameters in which the microscopic generalized displacement fluctuation field is decomposed in the membrane, bending and out-of-plane shear components.

For both KP and MP models, the aforementioned homogenization technique is followed and, by solving the internal static RVE equilibrium using a classical FE-procedure, the homogenized Σ and E quantities derived. Furthermore, the macro-stress couples are obtained by through-the-thickness integration of the homogeneous macro-stresses according to Eq. (11). The numerical integration is performed accounting only the mid-plane reference surface ω.

The obtained homogenized moment-curvature relations are defined per unit of length and so, if one intends to proceed with the micro-macro transition, a regularization step is required considering the macroscale mesh adopted.

$$M_{xx} = \int_{-z/2}^{z/2} \boldsymbol{\sigma}_{m,xx} z\,dz \;;\; M_{yy} = \int_{-z/2}^{z/2} \boldsymbol{\sigma}_{m,yy} z\,dz \;;\; M_{xy} = \int_{-z/2}^{z/2} \boldsymbol{\sigma}_{m,xy} z\,dz \qquad (11)$$

4.3 RVE definition and FE-modelling assumptions

The definition of the RVE being analysed at a micro-scale (within a two-step procedure) is required. It is generally accepted that the RVE may be statistically representative of the macro-scale level. It may contain a sufficient number of heterogeneities which possibly reproduce well the macro-behaviour [62] and are sufficiently small to respect the principle of scales separation of a first-order-homogenization theory. In the particular case of running- and English-bond masonry walls study, the choice of a proper RVE is somehow simplified due to the regular and periodic disposal of the constituent's arrangement. Even so, there are several RVE possibilities but, for both the analysed textures, the recommendation by Anthoine [14] is followed and presented in Figure 4.

In the modelling process, bricks are considered elastic and discretized as quadrilateral FE-plate elements with linear interpolation. A 2x2 Gauss-quadrature is adopted and three integration points are used in the thickness direction. Regarding the mortar joints, these are modelled as zero-thickness line interface elements which concentrate the material nonlinearity. Such a hypothesis seems to increase the efficiency of the framework by avoiding convergence issues related to distorted quadrilateral elements. However, the numerical consequences of using a strain-softening constitutive model may not be avoided, as stated next in the application section of the MP model.

A three-dimensional micro-model (direct numerical simulation, DNS model) is also developed. In order to allow a numerical comparison and draw consistent conclusions, the DNS model follows the same modelling assumptions, i.e. in terms of material properties, plasticity model for joints and mesh-size (in the plane).

5 Plasticity model for joint interfaces

Aiming at the decrease of the computational demand, material nonlinearity is assumed to be lumped on joints, as stated before. This assumption seems to be adequate for strong block masonry structures, once: (i) in absence or even in presence of small levels of any pre-compression state, cracking or crushing of bricks is unlikely to happen; (ii) the latter seems in agreement with experimental data, in which crack onset and propagation tend to follow a zigzag pattern along joints and between bricks [63,64].

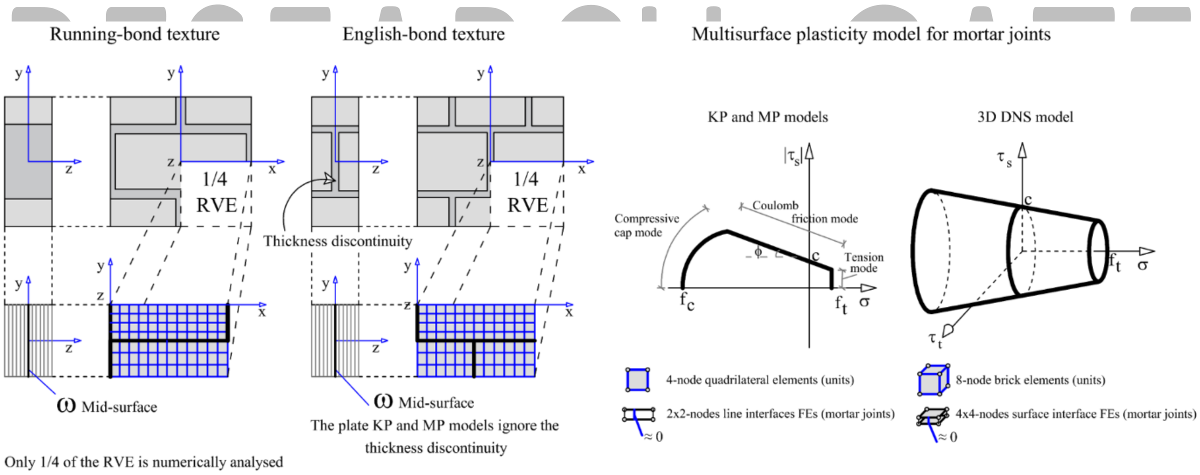

(a) (b)

Figure 4 – (a) The running- and English-bond masonry RVE considered for the KP, MP and DNS models; (b) Multi-surface plasticity model adopted for line [65] and surface interfaces [66].

A multi-surface plasticity model from Lourenço et. al. [65] (the so-called composite interface model) is considered for the interface elements used for the KP strategy. For the MP and DNS strategies, the model from by Van Zijl [66] is adopted, which is an extension of the latter to allow its use in a three-dimensional media, see Figure 4b. The plasticity models can well reproduce fracture, frictional slip and crushing along the interface elements. The constitutive interface model is defined by a convex composite yield criterion with three individual functions, i.e. a tension cut-off (Eq. 12) associated with a Mohr-Coulomb criterion (Eq. 13) is associated with and a cap in compression (Eq. 14). Softening behaviour is represented in all the modes. The tensile criterion (Figure 5a) reads:

$$f_t(\boldsymbol{\sigma}, \kappa_t) = \boldsymbol{\sigma} - \bar{\sigma}_t(\kappa_t) \text{ , and } \bar{\sigma}_t = f_t \exp\left(-\frac{f_t}{G_f^I}\kappa_t\right) \tag{12}$$

The shear criterion (Figure 5b) is given as:

$$f_s(\boldsymbol{\sigma}, \kappa_s) = |\tau| + \sigma tan\phi - \bar{\sigma}_s(\kappa_s) \text{ , and } \bar{\sigma}_s = c \exp\left(-\frac{c}{G_f^{II}}\kappa_s\right) \tag{13}$$

For the compressive yield function (Figure 5a):

$$f_c(\boldsymbol{\sigma}, \kappa_c) = {}^1/_2\,(\boldsymbol{\sigma}^T \boldsymbol{P} \boldsymbol{\sigma}) + \boldsymbol{p}^T \boldsymbol{\sigma} - \bar{\sigma}_c{}^2(\kappa_c) \tag{14}$$

Here, $\boldsymbol{\sigma}$ is the generalized stress, ϕ is the friction angle; $\boldsymbol{P}$ is a projection diagonal matrix and $\boldsymbol{p}$ a projection vector based on material parameters; G_f^I, G_f^{II} and G_f^{IV} are the mode-I, mode-II and the compressive fracture energy terms, respectively; $\bar{\sigma}_t$, $\bar{\sigma}_s$ and $\bar{\sigma}_c$ are the effective stresses of each of the adopted yield functions, governed by the internal scalar variables κ_t, κ_s and κ_c, respectively. Note that the typical compressive hardening/softening law $\bar{\sigma}_c(\kappa_c)$ is composed by three branches as observed in Figure 5c. The model follows the laws $\overline{\sigma_1}(\kappa_c), \overline{\sigma_2}(\kappa_c)$ and $\overline{\sigma_3}(\kappa_c)$ defined by Lourenço et. al. [65,66] which, for the sake of conciseness, are not exposed here and being the reader referred to [52,65,66] for further details.

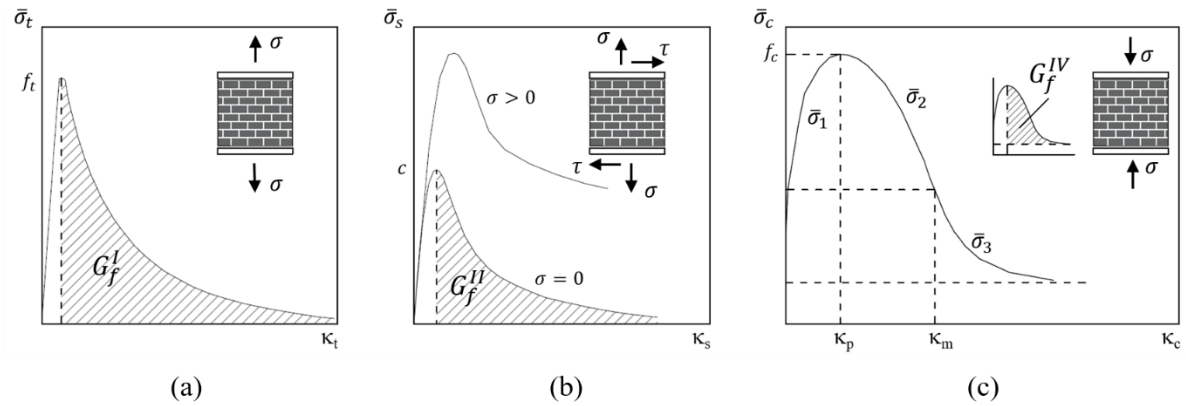

Figure 5 – Behaviour of quasi-brittle materials under: (a) tensile loading (mode-I, f_t is the tensile strength); (b) shear loading (mode-II, c is the cohesion) accounting with a potential pre-compression level; and (c) compressive load (f_c is the compressive strength; p and m are the peak and medium values, respectively).

6 Micro-mechanical validation: out-of-plane behaviour of masonry

The ability of the homogenization models to represent the out-of-plane behaviour of masonry is addressed next. Three main constitutive key features for numerical models aiming at the analysis of masonry are herein approached: (1) the correct representation of the elastic stiffness properties; (2) the masonry orthotropic behaviour due to the arrangement of the units; and (3) the role of vertical membrane pre-compression states, typically due to masonry self-weight and gravity loads in general.

6.1 Masonry homogenized elastic stiffness

The homogenized quantities of a running-bond masonry RVE, in terms of elastic stiffness components, are derived. The evaluation of the proposed KP and MP approaches is set through the results of a detailed FE micro-model and data from a simple closed-form solution by Zucchini and Lourenço [17]. A running bond RVE with dimensions equal to $210 \times 100 \times 52$ mm^3 and mortar joints of 10 mm of thickness is studied. The considered material elastic properties are the following ones: E_{brick}=20,000 MPa; ν_{brick}= 0.15; E_{joints}=E_{brick}/r and ν_{joints}= 0.15. The elastic homogenized stiffness parameters (Young and shear modulus) are assessed for several $r = E_{brick}/E_{mortar}$ ratios, ranging from 1 to 1000. Such broad range allows to represent the potential different stiffness ratios both in the elastic and in the inelastic range, in which the tangent and secant stiffness degradation of mortar joints occur.

An accurate detailed (interfaces explicitly modelled) FE micro-model (DNS model) is set as a reference. The use of this numerical model as a validation tool is clear, in fact, the elastic homogenized masonry stiffness calculation does not offer a complex problem nor novelty from a numerical standpoint. Such procedure is also convenient because a numerical study encompassing a wide range of components stiffness ratios is easily carried out. Reproducing the same data experimentally would require a thorough and expensive campaign. The obtained results are reported in Figure 6 and it can be observed how both the Kirchhoff-Love and Mindlin-Reissner plate models estimate well the elastic homogenized stiffness parameters. The agreement is, in general, very good according to the DNS model being the error less than 5%. Some differences may be found with the model proposed by Zucchini and Lourenço [17] especially for the shear modulus (see Figure 6b), but still, a good agreement is achieved with a micro-mechanical procedure based on a closed-form solution.

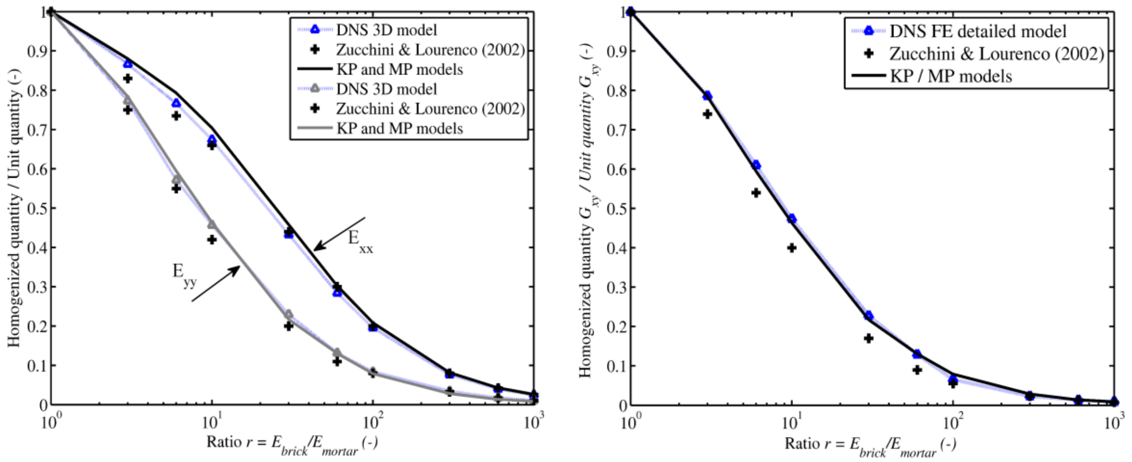

(a) (b)

Figure 6 – Comparison between the homogenized in-plane elastic properties obtained with a detailed FE micro-model (DNS 3D model), the KP and MP models and from the closed-form solution by Zucchini and Lourenço [17]: (a) Elastic Young modulus; (b) Shear modulus.

6.2 The masonry orthotropic behaviour: uni- and bi-axial bending

Masonry is known to present a well-marked anisotropic behaviour. The complexity increases because joints constitute planes of weakness which, depending on the stiffness ratio between mortar and brick constituents, may have a strong effect. Accounting for the non-linear behaviour of masonry is of prime importance as it can have an impact on the structural overall behaviour, energetic dissipation and mechanisms creation.

Two experimental campaign datasets are considered to validate the proposed homogenized models, i.e. the studies from van der Pluijm et al. [67] and Gazzola and Drysdale [68]. The former is herein firstly addressed and focus on the experimental test of several small panels in four-point bending, in which the bed joint angle with the normal assumes the values of 0, 30 and 90 degrees (defined as vertical, inclined and horizontal bending respectively). No pre-compression states are considered neither the post-peak information is available. Yet, both elastic limit and peak strength values are accessible within a curvature-bending moment diagram, which still constitutes a good source of information.

The panels were built with standard Dutch bricks, with dimensions 200×52×100 mm^3, and mortar joints with 10 mm of thickness. The elastic material properties assumed are the following ones: E_{brick}=11,000 MPa; ν_{brick}= 0.20; E_{joints}=4,000 MPa and ν_{joints}= 0.25. The inelastic mechanical parameters for mortar joint interfaces are given by f_t=0.25 MPa, G_f^I=0.006 N/mm, c=0.60 MPa, G_f^{II}=0.035 N/mm, ϕ=30 degrees, f_c=20.0 MPa and G_f^{IV}=4.00 N/mm. The latter values follow the average experimental values [67], and include missing parameters by inverse fitting.

The comparison between numerical and experimental results are summarized in Figure 7 in terms of curvature-bending moment curves. Data available from an elastic-plastic model for mortar joints by Milani and Tralli [44] is also used for comparison purposes. The different proposed homogenized procedures derive similar results. Thus, the three-dimensional shear effects seem to be negligible in this case, because the maximum relative difference found is about 3% (for the vertical bending moment peaks) between the DNS model and MP or KP models. One may also conclude that, despite the existent experimental data dispersion, the models reproduce well the orthotropy of masonry and its elastic bending stiffness. Still and regarding the latter, small differences are identified with the model proposed by Milani and Tralli [44] for the horizontal bending case. In fact, an elastic-plastic behaviour with softening for mortar joints is not so accurate in cases where a loss of the initial linear elastic stiffness occurs, as the one observed in the xx direction. In this way and in some cases, the initial calculated elastic bending stiffness may be not much representative. No further comparisons are addressed concerning the peak-bending moments because the authors adopted different fracture energies in tension, compression and shear regimes.

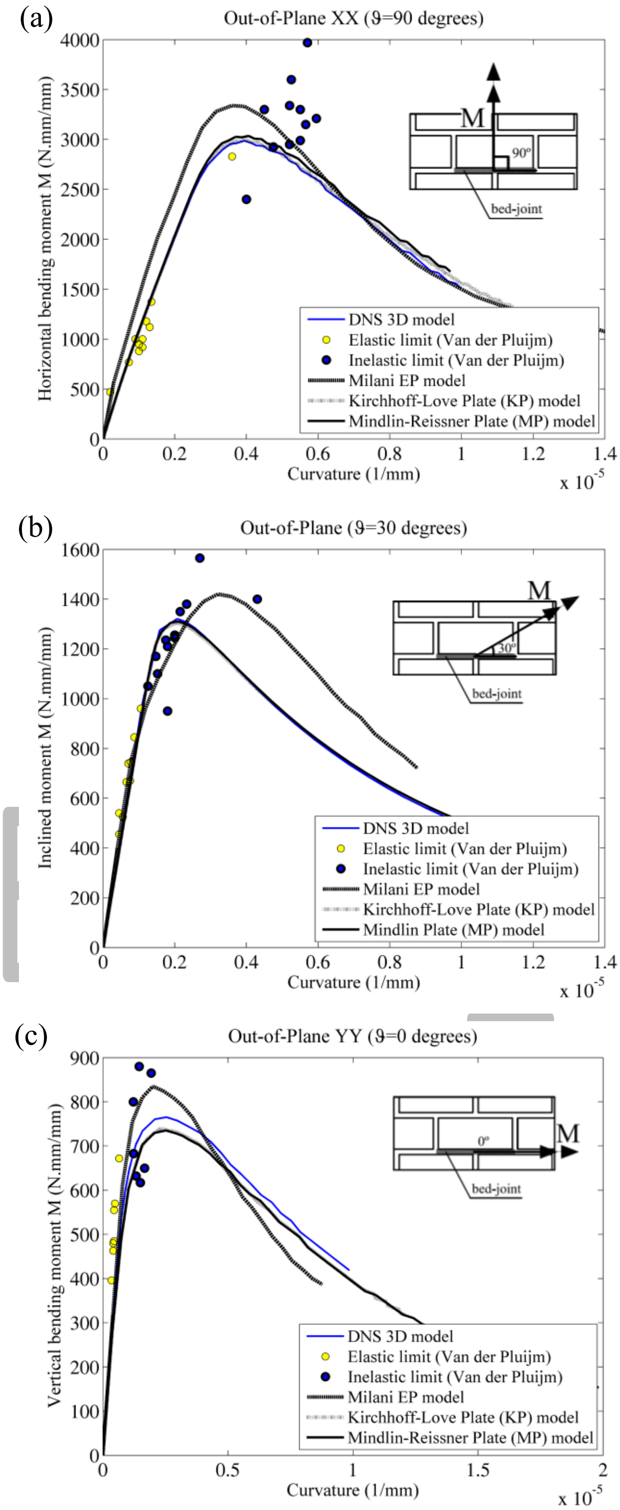

Figure 7 – Comparison between the experimental data from Van der Pluijm [67], the model from Milani and Tralli [44] and the numerical results obtained from the homogenized procedures proposed: (a) moment with a ϑ=90 degrees; (b) moment with a ϑ=0 degrees; and (c) moment with a ϑ=30 degrees.

The second set of experimental data used to study the material orthotropy behaviour derives from the Gazzola and Drysdale research [68,69]. This will be achieved by comparing the experimental set of peak flexural strength values, which represents a good indicator to analyse the orthotropic behaviour of masonry when subjected to out-of-plane loading and within a stepped or toothed failure pattern of masonry. The authors tested 25 wallets of hollow concrete block masonry, with different dimensions, within a running-bond texture in four-point bending. The bed joints angle with the loading direction ϑ were considered to vary between 0,15,45,75 and 90 degrees. The units' dimensions are 390×190×150 mm^3 and the mortar joints have a thickness equal to 10 mm. The elastic material properties assumed are the following: E_{brick}=10,000 MPa, v_{brick}= 0.20, E_{joints}=4,000 MPa, v_{joints}= 0.25; and the inelastic mechanical parameters for mortar joint interfaces are given by: f_t=0.20 MPa, G_f^I=0.018 N/mm, c=0.60 MPa, G_f^{II}=0.022 N/mm, ϕ=30 degrees, f_c=20.0 MPa and G_f^{IV}=4.00 N/mm. Only flexural strength peaks are at disposal and so the latter nonlinear material properties of mortar joints were tuned to fit the values of the horizontal ($\vartheta = 90$ degrees) and vertical ($\vartheta = 0$ degrees) flexural strengths, given by 0.92 MPa and 0.37 MPa respectively. The elastic material properties, even if assumed, are not relevant once these have a minor influence upon the moment capacity. The peak flexural strength is computed for each bed joint angle ϑ and the comparison between numerical and experimental data is showed in Figure 8.

No significant differences can be reported among the proposed homogenization approaches and, therefore, these are merged in Figure 8 as one dataset and labelled as *proposed homogenized models*. Additionally, information regarding the anisotropic macro-model by Lourenço [70], a simple elastic-plastic homogenized model by Casolo and Milani [44] and a kinematic-based homogenized model by Casolo and Milani [71] are also presented. It is possible to see that all the homogenized models seem capable to reproduce well the masonry orthotropy and provide accurate results.

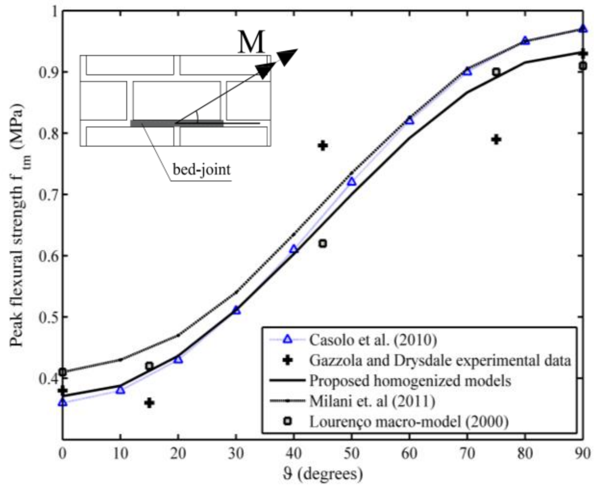

Figure 8 – Comparison between the experimental data from Gazzola and Drysdale [68] and the numerical results obtained from the proposed homogenized procedures.

6.3 The pre-compression state condition

The experimental program performed by Willis et al. [72] is herein used for a third and last validation key point, i.e. the ability to represent the effect of a vertical pre-compression state which is expected to increase both masonry moment capacity and ductility. A sample of twenty-five brickwork panels was subjected to horizontal bending, in which the load-deflection behaviour was collected for four levels of compressive stress σ_s (0.0075, 0.15 and 0.25 N/mm^2). The clay brick units have nominal dimensions of 230×65×114 mm^3 (length × height × thickness) and the mortar joints has 10 mm of thickness. The reader is referred to [72] for details about the experimental setup.

The experimental flexural tensile strengths are equal to 0.61-0.71 N/mm^2 (considered 0.70 N/mm^2) and 0.65 N/mm^2 for horizontal f_{th} and vertical f_{tv} bending, respectively. The adopted material properties were tuned to respect the latter values. The elastic properties are given as E_{brick}=10,000 MPa, ν_{brick}= 0.20, E_{joints}=2,000 MPa, ν_{joints}= 0.25; and the inelastic mechanical parameters for mortar joint interfaces given by: f_t=0.10 MPa, G_f^I=0.005 N/mm, c=0.18 MPa, G_f^{II}=0.02 N/mm, ϕ=30 degrees, f_c=20.0 MPa and G_f^{IV}=4.00 N/mm.

From the experimental data, it was possible to derive the full bending moment-curvature curve for a σ_S=0.15 N/mm^2. Figure 9 gathers the latter curve which allows the comparison with the derived numerical output. In any case, it is worth mentioning that the model is again able to reproduce quite well the orthotropic behaviour of masonry at failure in presence of weak mortar joints and toothed failure mechanisms.

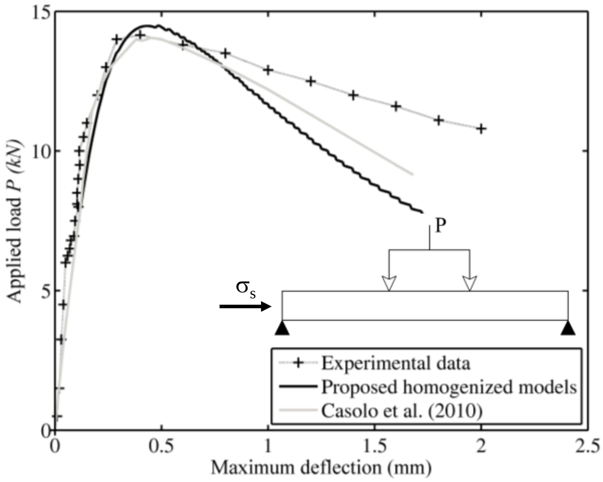

Figure 9 – Comparison between the experimental results from Willis et al. [72] and the numerical obtained with the proposed homogenized models and by the simplified model of Casolo and Milani [71].

6.4 Application: English-bond pattern

After the validation tests, the proposed homogenized models are extended to characterize the out-of-plane behaviour of an English bond masonry structure. The English-bond masonry benchmark was experimentally tested by Candeias et al. [73]. Here, only the geometry and the material properties of the masonry components are required and described.

The majority of the existing research on masonry deal with running-bond texture within a single-wythe walls case [12,17,18,39,48]. The analysis of the effect of potential discontinuities on the masonry thickness, when two- or three-wythes of masonry are present, the effect of three-dimensional shear stresses and the study of other periodic textures, as the English-bond, are somehow under-investigated.

Still, some studies can be reported. In the particular level of simplified multi-scale methods, Casolo and Milani [47] studied the behaviour of three-leaf masonry walls and proposed, at a micro-scale, two simple unit cell homogenization models to compute the out-of-plane homogenized quantities. One is an FE-based procedure, where bricks are assumed to be elastic and joints are reduced to interface elements, and the other is based on an analytical approach. Even if both are accurate and relatively fast, it is found that the former does not consider the softening behaviour of interfaces and the latter to be an ad-hoc procedure thus demanding its extension to other components arrangements. Moreover, Cecchi and Milani [51] characterized the micro-scale behaviour of an English-bond masonry wall through a simple homogenization model. Masonry units are considered as rigid blocks and joints modelled as 2D Reissner-Mindlin plate elements to conceive the model the ability to explicitly reproduce the out-of-plane shear effects. Still, conclusions upon its influence are drawn at a structural level only through the comparison with a full-FE micro-model. It may also be noteworthy to mention the research from Massart et al. [74] in the field of full-FE homogenization approaches. Even if applied to a running-bond masonry and within in-plane loading case, three-dimensional effects are reproduced through the implementation of a two-dimensional generalised plane state formulation.

In this context, the experimental study upon an English-bond masonry structure benchmark [73] constitutes an important step. The data may encourage and drive the studies of different numerical strategies towards the better understanding of the latter effects. Accordingly, the current analysis tries to conclude about the effect of three-dimensional shear stresses and the role played by joints discontinuities along the thickness direction.

An English-bond masonry RVE is analysed, see Figure 4a. The brick units have in-plane dimensions of 235x70x115 mm^3 (length x height x thickness) and the bed and head mortar joints have a thickness $t_{joint} = 15mm$. When laid and bound together in an English-bond texture the wall yields a thickness of 235 mm. The mechanical properties adopted are collected in Table 1 and follow the values available both from experimental data and literature studies which adopted the same benchmark [73]. Note that the linear elastic relation between the generalized stresses and strains of the interface FEs is given by the classical constitutive equation $\boldsymbol{\sigma} = \boldsymbol{D}\boldsymbol{\varepsilon}$. Considering a line FE interface (for the adopted plate theories KP and MP models), the elastic stiffness matrix $\boldsymbol{D}$ is given as $D = diag\{k_n, k_s\}$. The values of the normal (k_n) and shear (k_s) mortar joints stiffness terms can be easily computed. One possibility is to neglect the contribution of the brick-mortar interface and to compute these parameters as $k_n = E_{mortar}/t_{joint}$ and $k_s = G_{mortar}/t_{joint}$, where G_{mortar} is the mortar shear modulus. Another possibility is to follow the suggestions given in [75] in which, under the assumption of a stack bond where a serial chain connection represents the masonry components (with uniform stress distributions in both unit and mortar joints), the latter stiffnesses' values read:

$$k_n = \frac{E_{brick}E_{mortar}}{t_{joint}(E_{brick} - E_{mortar})} \tag{15}$$

$$k_s = \frac{G_{brick}G_{mortar}}{t_{joint}(G_{brick} - G_{mortar})} \tag{16}$$

Equations (15) and (16) are typically considered [76] and are employed in this study (see Table 1). It may be highlighted that a penalty approach is not followed by the adopted interface FEs [76] to phenomenologically represent the behaviour of masonry crushing. Such strategy is usually adopted in discrete element models [3,4], or advanced FE software's able to model discrete rigid bodies (e.g. [77]), to guarantee an appropriate physical contact between units. Here, penetration and overlapping between neighbouring brick units can occur which does not blur the accuracy of the in- and out-of-plane quantities derived; particularly if addressed that a weak mortar masonry is being studied and so low compressive levels of stress are expected.

Four values are considered for the RVE thickness, namely *t=470 mm*, *t=235 mm*, *t=141 mm* and *t=70.5 mm*. The results obtained with the simulations from the KP and MP models are compared with the ones derived with a three-dimensional micro-model (DNS model), as done for the previous validation steps, and depicted in Figure 10. Several conclusions can be put together. Firstly, and as expected, no considerable differences regarding the peak moments (M_{xx}, M_{yy}, M_{xy}) are found, between the MP and the DNS models, for all the studied thicknesses. The MP model is able to capture well the out-of-plane shear effects. Yet, it is important to recall that for the MP model, with the increase of the thickness value, the post-peak curves are not so well developed due to convergence issues as demonstrated in Figure 10.

Table 1 – Material properties adopted for the English bond masonry [73].

Elastic Properties		Elastic and Inelastic Properties									
Brick units		Mortar joints									
E_{units}	υ	E_{mortar}	k_n	k_s	f_t	f_c	c	G_f^I	G_f^{II}	G_f^{IV}	φ
11,000 N/mm²	0.25 (-)	2,200 *N/mm²*	183 *N/mm*	72.6 *N/mm*	0.105 *N/mm²*	2.84 *N/mm²*	0.20 *N/mm²*	0.012 *N/mm*	0.05 *N/mm*	3.97 *N/mm*	30º

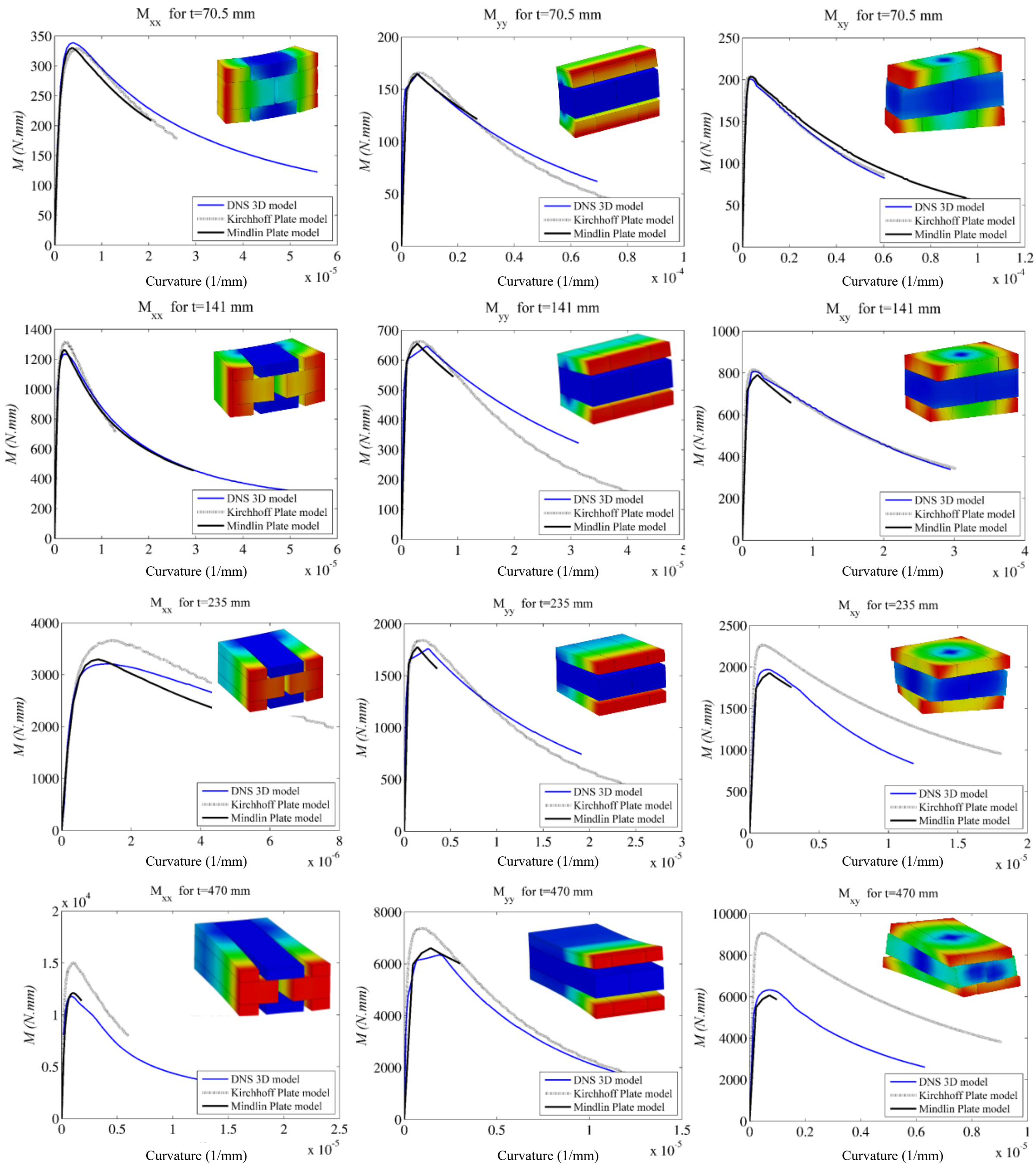

Figure 10 – Numerical results obtained with the proposed numerical strategies for the English-bond masonry texture for the four RVE thickness values defined.

The authors experienced some convergence problems in developing the post-peak branch due to snap-back issues. It is known that when interface elements employ a softening type of damage model convergence problems can be experienced after the cracking onset and propagation [78,79]. Even if a cylindrical arc-length procedure including a line search algorithm is active the solution fails which, in theory, leads to the requirement of improved arc-length techniques, see [80], or the imposition of constraints equations upon the interface nodes [79].

Conversely, no convergence issues are reported for the KP model. This is based on an in-plane identification within a plane-stress formulation, from which the out-of-plane quantities are simply obtained through on-thickness integration. The computational time required by the KP model to derive all the in- and out-of-plane homogenized quantities (Σ_{xx}, Σ_{xy}, Σ_{yy}, M_{xx}, M_{xy}, M_{yy}) is around 81 seconds, which is significantly less than the three-dimensional DNS (246 seconds) and MP (154 seconds) models. So, the KP model seems the most suitable procedure to be integrated within a full automatic FE^2 procedure, albeit its inability to reproduce the out-of-plane shear stresses can lead to considerable errors depending on the thickness of the RVE being analysed. Figure 10 clearly shows the latter where, for a thickness of 235 mm (real dimensions) and 470 mm, an error of 14% and 23% is found, respectively. Another important feature is that the observed differences in the peak moment values are especially critical for both M_{xx} and M_{xy} and not relevant for the vertical bending M_{yy}. This exception is easily understandable from a physical standpoint. Bearing that for M_{yy} a typical de-bonding failure is achieved, see Figure 3a, this is mainly dependent on the tensile strength value of the horizontal joints being the shear effect of the vertical interfaces irrelevant.

To what concerns the effect of the mid-thickness vertical joint existing on the English-bond masonry walls, two DNS models are considered. One does not take into account the discontinuity along the thickness; the other considers it, explicitly modelled and with a thickness of 17 mm. Figure 11 shows the obtained results. Due to the aforementioned stated reasons, the presence of the discontinuity has a marginal effect on the vertical bending behaviour M_{yy} of the RVE. In opposition, the model with the discontinuity manifests a lower capacity for both horizontal M_{xx} and torsional M_{xy} moments, with differences ranging 33% and

17%, respectively. Additionally, if the KP model results are considered, an error of 52% is expected for the horizontal bending moment case. Such results prove how important is to address the existence of masonry discontinuities along the thickness and the need that may be required when choosing the modelling strategy for a given study case.

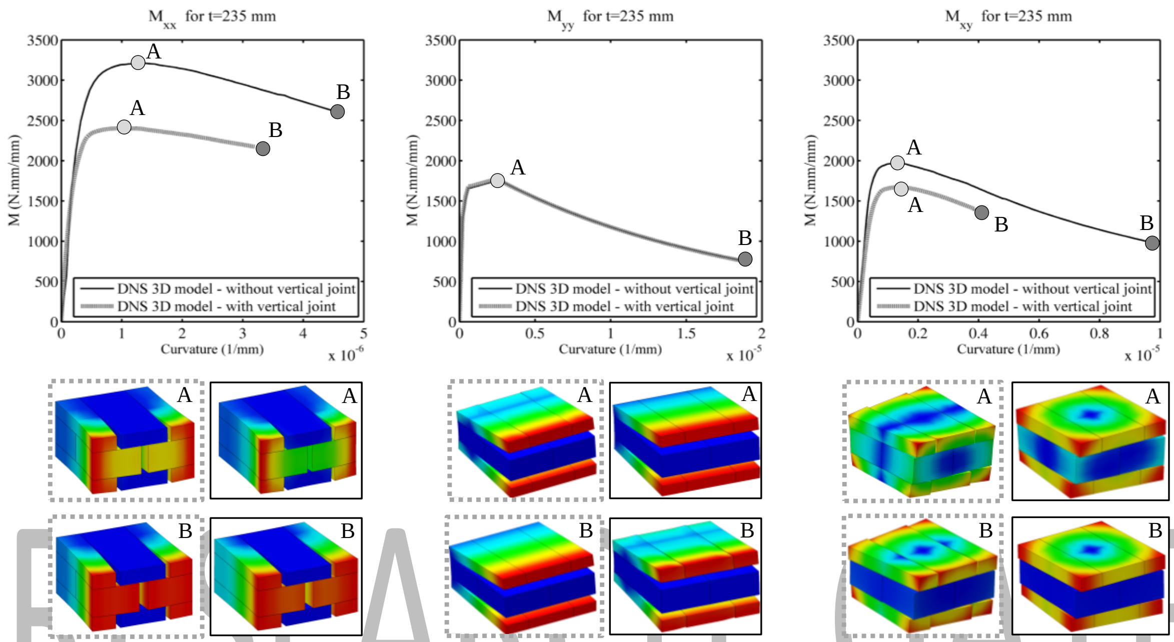

Figure 11 – Comparison between the results obtained for the three bending components via a 3D DNS model considering and non-considering the existent vertical joint on the mid-thickness of the English-bond masonry.

7 Conclusions

Two microscopic FE-models based on a first-order homogenization theory and within a strain-driven formulation were formulated to characterize the behaviour of masonry. A Kirchhoff-Love and Mindlin-Reissner plate theory were adopted. These have been designated in the paper as KP and MP models, respectively. In both strategies, a representative volume element (RVE), aimed at representing masonry by repetition, was modelled through the assemblage of quadrilateral elements with linear interpolation for bricks and line interface elements with zero-thickness for mortar joints. By solving a BVP upon the defined RVE, both the in-plane stresses and out-of-plane stress-couples were derived from the microscopic level.

With bricks assumed to be elastic and with interface elements carrying the inelastic material information within a multi-surface plasticity model [65] (an assumption plausible for strong blocks), a stepped, toothed and a de-bonding masonry failure patterns were suitably reproduced.

The validation of the KP and MP models was performed first at a micro-level. Available experimental data together with the results obtained via a three-dimensional micro-mechanical model (DNS model) were used as reference. Three main constitutive key features were addressed: (1) the correct representation of the elastic stiffness properties [17]; (2) the masonry orthotropic behaviour due to the arrangement of the units [67,68]; and (3) the role of vertical membrane pre-compression states [72]. The validation proved to work well for all the three steps, with homogenized results fitting with excellent accuracy the reference data.

The application of the microscopic FE-homogenized based models was carried out for a real case study of an English-bond masonry mock-up tested by Candeias et al. [81]. The analyses were performed using data derived numerically, namely the homogenized out-of-plane quantities M_{xx}, M_{xy} and M_{yy}, which clearly depend on the in-plane behaviour of the masonry. Four values for the RVE thickness were adopted aiming at studying the out-of-plane shear stresses effect. The MP model follows an out-of-plane shear deformation theory and thus was able to provide similar results to the ones from the DNS model. The simplified KP model proved good accuracy for the cases where the thickness has a value which is similar or lower than the RVE dimensions (i.e. its height or length). It is worth noting that the KP strategy allows faster computations with no-convergence issues reported. Insomuch, in order to test the effect of the presence of a mortar layer on the RVE thickness (present in an English-bond texture) two micro-models were further analysed. The conclusions demonstrate that the discontinuity plays an important role in the decrease of the horizontal bending (around 33%)

and torsional moment capacities (around 17%), whereas the influence on vertical bending is minimal.

The above micro-mechanical homogenized-based models are characterized by several advantages, mainly related with their versatility. By exploiting the use of plate theory assumptions, the strategies allow replacing the three-dimensional microscopic continuum into a two-dimensional one. Such procedures are thus quite convenient, due to the simplicity of application, accuracy and low computational effort required. Moreover, these are suitable to be integrated within a FE^2 approach, especially with simplified discrete methods at a macro-scale as [44,46,82]. Still, two issues can be raised. At a micro-scale the damage evolution is restricted to the mortar joints and so a regularization is not needed. However, the use of the previous macro-models based on rigid plates lead to an intrinsic mesh dependence, specifically to what concerns with the localization of the inelastic strains. This is a consequence of the simplicity and robustness of these approaches (see [44] for a more detailed insight). It is certainly possible to embed more discontinuities or regularization strategies in the macroscopic model, for instance using a non-local model implementable, in practice, by connecting non-adjoining elements with additional springs. Nevertheless, this is not the primary objective when selecting such type of simplified procedures, instead these are meant to largely decrease the processing running times at a structural level. It is the authors' opinion that if the homogenised models are implemented within the latter macro-discrete FE models (see [43,44,46,82]) or a related strategy, the feasibility of its application for the study of large-scale structures and in the scope of dynamic problems is well assured.

As further developments to this study, the authors outline four possibilities: (1) to draw more general conclusions, additional analyses can be carried out with different geometric dimensions for both the RVE components (bricks and mortar joints) and the wall thickness; (2) unit-unit interface FEs can be modelled to allow reproducing the splitting failure of bricks; (3) the homogenized models can also extended to other periodic masonry arrangements or even adapted to study irregular textures; and (4) if a proper kinematical map is developed to deal with the transition between the two-scales, these may also be used within a nested full-FE-continuous approach.

Acknowledgements

This work was supported by FCT (Portuguese Foundation for Science and Technology), within ISISE, scholarship SFRH/BD/95086/2013. This work was also partly financed by FEDER funds through the Competitivity Factors Operational Programme - COMPETE and by national funds through FCT – Foundation for Science and Technology within the scope of the project POCI-01-0145-FEDER-007633.

References

[1] Lourenço PB. Recent advances in masonry structures: Micromodelling and homogenisation. In: Galvanetto U, Aliabadi MHF, editors. Multiscale Model. Solid Mech., vol. 3, Imperial College Press; 2009, p. 251–94. doi:10.1142/p604.

[2] Lourenço PB. Computations on historic masonry structures. Prog Struct Eng Mater 2002;4:301–19. doi:10.1002/pse.120.

[3] Sarhosis V, Bagi K, Lemos J V., Milani G, editors. Computational Modeling of Masonry Structures Using the Discrete Element Method. IGI Global; 2016. doi:10.4018/978-1-5225-0231-9.

[4] Lemos J V. Discrete Element Modeling of Masonry Structures. Int J Archit Herit 2007;1:190–213. doi:10.1080/15583050601176868.

[5] Feyel F, Chaboche J-L. FE2 multiscale approach for modelling the elastoviscoplastic behaviour of long fibre SiC/Ti composite materials. Comput Methods Appl Mech Eng 2000;183:309–30. doi:10.1016/S0045-7825(99)00224-8.

[6] Miehe C, Koch A. Computational micro-to-macro transitions of discretized microstructures undergoing small strains. Arch Appl Mech (Ingenieur Arch 2002;72:300–17. doi:10.1007/s00419-002-0212-2.

[7] Kouznetsova V, Brekelmans WAM, Baaijens FPT. An approach to micro-macro modeling of heterogeneous materials. Comput Mech 2001;27:37–48. doi:10.1007/s004660000212.

[8] Spahn J, Andrä H, Kabel M, Müller R. A multiscale approach for modeling progressive damage of composite materials using fast Fourier transforms. Comput Methods Appl Mech Eng 2014;268:871–83. doi:10.1016/j.cma.2013.10.017.

[9] Yamanaka T, Ghiasi H, Heidari-Rarani M, Lessard L, Feret V, Hubert P. Multiscale finite element analysis of mode I delamination growth in a fabric composite. Compos

Struct 2015;133:157–65. doi:10.1016/j.compstruct.2015.07.094.
[10] Mercatoris BCN, Massart TJ. A coupled two-scale computational scheme for the failure of periodic quasi-brittle thin planar shells and its application to masonry. Int J Numer Methods Eng 2011;85:1177–206. doi:10.1002/nme.3018.
[11] van den Eijnden AP, Bésuelle P, Chambon R, Collin F. A FE2 modelling approach to hydromechanical coupling in cracking-induced localization problems. Int J Solids Struct 2016;97–98:475–88. doi:10.1016/j.ijsolstr.2016.07.002.
[12] Pande GN, Liang JX, Middleton J. Equivalent elastic moduli for brick masonry. Comput Geotech 1989;8:243–65. doi:10.1016/0266-352X(89)90045-1.
[13] Papa E. A unilateral damage model for masonry based on a homogenisation procedure. Mech Cohesive-Frictional Mater 1996;1:349–66. doi:10.1002/(SICI)1099-1484(199610)1:4<349::AID-CFM18>3.0.CO;2-M.
[14] Anthoine A. Derivation of the in-plane elastic characteristics of masonry through homogenization theory. Int J Solids Struct 1995;32:137–63. doi:10.1016/0020-7683(94)00140-R.
[15] Luciano R, Sacco E. Homogenization technique and damage model for old masonry material. Int J Solids Struct 1997;34:3191–208. doi:10.1016/S0020-7683(96)00167-9.
[16] Mistler M, Anthoine A, Butenweg C. In-plane and out-of-plane homogenisation of masonry. Comput Struct 2007;85:1321–30. doi:10.1016/j.compstruc.2006.08.087.
[17] Zucchini A, Lourenço P. A micro-mechanical model for the homogenisation of masonry. Int J Solids Struct 2002;39:3233–55. doi:10.1016/S0020-7683(02)00230-5.
[18] Milani G, Lourenço P, Tralli A. 3D homogenized limit analysis of masonry buildings under horizontal loads. Eng Struct 2007;29:3134–48. doi:10.1016/j.engstruct.2007.03.003.
[19] Otero F, Oller S, Martinez X, Salomón O. Numerical homogenization for composite

materials analysis. Comparison with other micro mechanical formulations. Compos Struct 2015;122:405–16. doi:10.1016/j.compstruct.2014.11.041.

[20] Ghosh S, Lee K, Moorthy S. Multiple scale analysis of heterogeneous elastic structures using homogenization theory and voronoi cell finite element method. Int J Solids Struct 1995;32:27–62. doi:10.1016/0020-7683(94)00097-G.

[21] Smit RJM, Brekelmans WAM, Meijer HEH. Prediction of the mechanical behavior of nonlinear heterogeneous systems by multi-level finite element modeling. Comput Methods Appl Mech Eng 1998;155:181–92. doi:10.1016/S0045-7825(97)00139-4.

[22] Valenta R, Sejnoha M, Zeman J. Macroscopic Constitutive Law for Mastic Asphalt Mixtures from Multiscale Modeling. Int J Multiscale Comput Eng 2010;8:131–49. doi:10.1615/IntJMultCompEng.v8.i1.100.

[23] Sýkora J, Šejnoha M, Šejnoha J. Homogenization of coupled heat and moisture transport in masonry structures including interfaces. Appl Math Comput 2013;219:7275–85. doi:https://doi.org/10.1016/j.amc.2011.02.050.

[24] Bažant ZP, Oh BH. Crack band theory for fracture of concrete. Matériaux Constr 1983;16:155–77. doi:10.1007/BF02486267.

[25] Geers MGD, Kouznetsova VG, Brekelmans WAM. Multi-scale computational homogenization: Trends and challenges. J Comput Appl Math 2010;234:2175–82. doi:10.1016/j.cam.2009.08.077.

[26] Petracca M, Pelà L, Rossi R, Oller S, Camata G, Spacone E. Regularization of first order computational homogenization for multiscale analysis of masonry structures. Comput Mech 2016;57:257–76. doi:10.1007/s00466-015-1230-6.

[27] Silva LC, Lourenço PB, Milani G. Rigid block and spring homogenized model (HRBSM) for masonry subjected to impact and blast loading. Int J Impact Eng 2017;109:14–28. doi:10.1016/j.ijimpeng.2017.05.012.

[28] Kouznetsova VG, Geers MGD, Brekelmans WAM. Multi-scale second-order computational homogenization of multi-phase materials: a nested finite element solution strategy. Comput Methods Appl Mech Eng 2004;193:5525–50. doi:10.1016/j.cma.2003.12.073.

[29] Bacigalupo A, Gambarotta L. Computational two-scale homogenization of periodic masonry: Characteristic lengths and dispersive waves. Comput Methods Appl Mech Eng 2012;213–216:16–28. doi:10.1016/j.cma.2011.11.020.

[30] Forest S, Pradel F, Sab K. Asymptotic analysis of heterogeneous Cosserat media. Int J Solids Struct 2001;38:4585–608. doi:10.1016/S0020-7683(00)00295-X.

[31] Casolo S. Macroscopic modelling of structured materials: Relationship between orthotropic Cosserat continuum and rigid elements. Int J Solids Struct 2006;43:475–96. doi:10.1016/j.ijsolstr.2005.03.037.

[32] Addessi D, Sacco E, Paolone A. Cosserat model for periodic masonry deduced by nonlinear homogenization. Eur J Mech - A/Solids 2010;29:724–37. doi:10.1016/j.euromechsol.2010.03.001.

[33] Moulinec H, Suquet P. A numerical method for computing the overall response of nonlinear composites with complex microstructure. Comput Methods Appl Mech Eng 1998;157:69–94. doi:10.1016/S0045-7825(97)00218-1.

[34] Vondřejc J, Zeman J, Marek I. An FFT-based Galerkin method for homogenization of periodic media. Comput Math with Appl 2014;68:156–73. doi:10.1016/j.camwa.2014.05.014.

[35] Hashin Z, Rosen BW. The Elastic Moduli of Fiber-Reinforced Materials. J Appl Mech 1964;31:223–32.

[36] Dvorak GJ, Teply JL. Periodic Hexagonal Array Models for Plasticity of Composite Materials. Plast. Today Model. Methods Appl., vol. W. Olszak, Elsevier Science

Publishers B. V.; 1985, p. 623–42.

[37] Aboudi J. Mechanics of composite materials: a unified micromechanical approach. 1991.

[38] Drougkas A, Roca P, Molins C. Analytical micro-modeling of masonry periodic unit cells – Elastic properties. Int J Solids Struct 2015;69:169–88. doi:10.1016/j.ijsolstr.2015.04.039.

[39] Taliercio A. Closed-form expressions for the macroscopic in-plane elastic and creep coefficients of brick masonry. Int J Solids Struct 2014;51:2949–63. doi:10.1016/j.ijsolstr.2014.04.019.

[40] Ghosh S, Lee K, Raghavan P. A multi-level computational model for multi-scale damage analysis in composite and porous materials. Int J Solids Struct 2001;38:2335–85. doi:10.1016/S0020-7683(00)00167-0.

[41] Lloberas-Valls O, Rixen DJ, Simone A, Sluys LJ. On micro-to-macro connections in domain decomposition multiscale methods. Comput Methods Appl Mech Eng 2012;225–228:177–96. doi:10.1016/j.cma.2012.03.022.

[42] Greco F, Leonetti L, Luciano R, Nevone Blasi P. An adaptive multiscale strategy for the damage analysis of masonry modeled as a composite material. Compos Struct 2016;153:972–88. doi:10.1016/j.compstruct.2016.06.066.

[43] Milani G, Lourenço PB, Tralli A. Homogenised limit analysis of masonry walls, Part II: Structural examples. Comput Struct 2006;84:181–95. doi:10.1016/j.compstruc.2005.09.004.

[44] Milani G, Tralli A. Simple SQP approach for out-of-plane loaded homogenized brickwork panels, accounting for softening. Comput Struct 2011;89:201–15. doi:10.1016/j.compstruc.2010.09.005.

[45] Milani G, Venturini G. Automatic fragility curve evaluation of masonry churches

accounting for partial collapses by means of 3D FE homogenized limit analysis. Comput Struct 2011;89:1628–48. doi:10.1016/j.compstruc.2011.04.014.

[46] Silva LC, Lourenço PB, Milani G. Nonlinear Discrete Homogenized Model for Out-of-Plane Loaded Masonry Walls. J Struct Eng 2017;143. doi:10.1061/(ASCE)ST.1943-541X.0001831.

[47] Casolo S, Milani G. Simplified out-of-plane modelling of three-leaf masonry walls accounting for the material texture. Constr Build Mater 2013;40:330–51. doi:10.1016/j.conbuildmat.2012.09.090.

[48] Lee JS, Pande GN, Middleton J, Kralj B. Numerical modelling of brick masonry panels subject to lateral loadings. Comput Struct 1996;61:735–45. doi:10.1016/0045-7949(95)00361-4.

[49] Ghiassi B, Soltani M, Tasnimi AA. A simplified model for analysis of unreinforced masonry shear walls under combined axial, shear and flexural loading. Eng Struct 2012;42:396–409. doi:https://doi.org/10.1016/j.engstruct.2012.05.002.

[50] Ghiassi B, Soltani M, Tasnimi AA. Seismic Evaluation of Masonry Structures Strengthened with Reinforced Concrete Layers. J Struct Eng 2012;138:729–43. doi:10.1061/(ASCE)ST.1943-541X.0000513.

[51] Cecchi A, Milani G. A kinematic FE limit analysis model for thick English bond masonry walls. Int J Solids Struct 2008;45:1302–31. doi:10.1016/j.ijsolstr.2007.09.019.

[52] DIANA. User’s manual 2017.

[53] Suquet PM. Elements of Homogenization for Inelastic Solid Mechanics. Homog. Tech. Compos. media, Springer-Verlag; 1987, p. 193–278.

[54] Blanco PJ, Sánchez PJ, de Souza Neto EA, Feijóo RA. Variational Foundations and Generalized Unified Theory of RVE-Based Multiscale Models. Arch Comput Methods Eng 2016;23:191–253. doi:10.1007/s11831-014-9137-5.

[55] Milani G, Lourenço P, Tralli A. Homogenization Approach for the Limit Analysis of Out-of-Plane Loaded Masonry Walls. J Struct Eng 2006;132:1650–63. doi:10.1061/(ASCE)0733-9445(2006)132:10(1650).

[56] Cecchi A, Sab K. Out of plane model for heterogeneous periodic materials: the case of masonry. Eur J Mech - A/Solids 2002;21:715–46. doi:10.1016/S0997-7538(02)01243-3.

[57] Cecchi A, Milani G, Tralli A. A Reissner–Mindlin limit analysis model for out-of-plane loaded running bond masonry walls. Int J Solids Struct 2007;44:1438–60. doi:10.1016/j.ijsolstr.2006.06.033.

[58] Hughes TJR, Tezduyar TE. Finite Elements Based Upon Mindlin Plate Theory With Particular Reference to the Four-Node Bilinear Isoparametric Element. J Appl Mech 1981;48:587. doi:10.1115/1.3157679.

[59] E. Reissner. On transverse bending of plates, including the effect of transverse shear deformation. Int J Solids Struct 1975;11:569–73. doi:10.1016/0020-7683(75)90030-X.

[60] Zienkiewicz OC, Taylor RL. The Finite Element Method: Solid mechanics. (Vol. 2). Butterworth-Heinemann; 2000.

[61] Arnold DN, Madureira AL, Zhang S. On the Range of Applicability of the Reissner–Mindlin and Kirchhoff–Love Plate Bending Models. J Elast 2002;67:171–85. doi:10.1023/A:1024986427134.

[62] Hill R. A self-consistent mechanics of composite materials. J Mech Phys Solids 1965;13:213–22. doi:10.1016/0022-5096(65)90010-4.

[63] Sinha BP. A Simplified ultimate load analysis of laterally-loaded model orthotropic brickwork panels of low tensile strength. Struct Eng ASCE 1978;56B:81–4.

[64] Herbert DM, Gardner DR, Harbottle M, Hughes TG. Uniform lateral load capacity of small-scale masonry wall panels. Mater Struct 2014;47:805–18. doi:10.1617/s11527-

013-0092-7.

[65] Lourenço PB, Rots JG. Multisurface Interface Model for Analysis of Masonry Structures. J Eng Mech 1997;123:660–8. doi:10.1061/(ASCE)0733-9399(1997)123:7(660).

[66] Zijl, Van GPAG. Computational Modelling of Masonry Creep and Shrinkage. Delft University of Technology, 2000.

[67] Pluijm van der RR. Out-of-plane bending of masonry: behaviour and strength. Doctoral dissertation, Technische Universiteit Eindhoven, 1999.

[68] Gazzola EA, Drysdale RG, Essawy AS. Bending of concrete masonry walls at different angles to the bed joints. Proc. 3rd North Am. Mason. Conf., 1985.

[69] Gazzola EA, Drysdale RG. A Component Failure Criterion for Blockwork in Flexure. Adv. Anal. Struct. Mason., ASCE; 1986, p. 134–54.

[70] Lourenço PB. Anisotropic Softening Model for Masonry Plates and Shells. J Struct Eng 2000;126:1008–16. doi:10.1061/(ASCE)0733-9445(2000)126:9(1008).

[71] Casolo S, Milani G. A simplified homogenization-discrete element model for the non-linear static analysis of masonry walls out-of-plane loaded. Eng Struct 2010;32:2352–66. doi:10.1016/j.engstruct.2010.04.010.

[72] Willis CR, Griffith MC, Lawrence SJ. Horizontal Bending of Unreinforced Clay Brick Masonry. Mason Int 2004;17:109–21.

[73] Mendes N, Lourenço PB, Campos-Costa A. Shaking table testing of an existing masonry building: assessment and improvement of the seismic performance. Earthq Eng Struct Dyn 2014;43:247–66. doi:10.1002/eqe.2342.

[74] Massart TJ, Peerlings RHJ, Geers MGD, Gottcheiner S. Mesoscopic modeling of failure in brick masonry accounting for three-dimensional effects. Eng Fract Mech 2005;72:1238–53. doi:10.1016/j.engfracmech.2004.09.007.

[75] CUR. Structural masonry: a experimental/numerical basis for practical design rules (in Dutch) 1994;Report 171.

[76] Lourenço PB. Computational strategies for masonry structures. PhD Thesis. Delft University of Technology, Delft, The Netherlands, 1996.

[77] ABAQUS. Finite Element Analysis (Theory manual). Providence: RI: Dassault Systèmes Simulia Corporation; 2013.

[78] Hellweg H-B, Crisfield MA, Davies GAO. Failure analysis of composite structures using interface elements. In: Eggington RE, editor. NAFEMS Conf. Appl. Finite Elem. to Compos. Mater., 1994, p. 6–9.

[79] De Borst R. Computation of post-bifurcation and post-failure behavior of strain-softening solids. Comput Struct 1987;25:211–24. doi:10.1016/0045-7949(87)90144-1.

[80] Hellwega H-B, Crisfield MA. A new arc-length method for handling sharp snap-backs. Comput Struct 1998;66:704–9. doi:10.1016/S0045-7949(97)00077-1.

[81] Candeias PX, Costa AC, Mendes N, Costa AA, Lourenço PB. Experimental Assessment of the Out-of-Plane Performance of Masonry Buildings Through Shaking Table Tests. Int J Archit Herit 2016:1–28. doi:10.1080/15583058.2016.1238975.

[82] Casolo S. Rigid element model for non-linear analysis of masonry façades subjected to out-of-plane loading. Commun Numer Methods Eng 1999;15:457–68.